EXPERIMENTAL RESULTS OF A 10 KW_E ORGANIC RANKINE CYCLE WITH A VARIABLE VOLUME RATIO EXPANDER

Couvreur K.*, Tassenoy R., van Heule X., De Paepe M. and Lecompte S.
*Author for correspondence
Department of Electromechanical, Systems and Metal Engineering,
Ghent University,
Ghent, 9000,
Belgium,
E-mail: Kenny.Couvreur@UGent.be

ABSTRACT

In this paper the experimental results of a 10 kWe prototype organic Rankine cycle (ORC) to be integrated in a Carnot battery is presented. The reciprocating piston expander used in this work has a built-in mechanism which allows changing the inlet valve timing of the expander and hence the expander internal volume - and pressure ratio. A total of 58 steady state points have been collected by varying the heat source and cold sink temperature, the refrigerant mass flow rate, the expander speed and the expander inlet valve timing. The experimental results for the ORC are presented in terms of electrical power output and cycle efficiency and for the expander the isentropic and volumetric efficiencies are determined for different valve timings. This study demonstrates the optimization potential of variable volume ratio reciprocating piston expanders used in ORC's which experience varying external conditions.

NOMENCLATURE

c	[J/kg.K]	Specific heat
FF	[%]	Filling factor
h	[J/kg]	Specific enthalpy
$\dot{m}$	[kg/s]	Mass flow rate
p	[Pa]	Pressure
PR	[-]	Pressure ratio
$\dot{Q}$	[W]	Heat rate
r_v	[-]	Built in volume ratio
s	[J/K]	Specific entropy
T	[°C]	Temperature
V	[m³]	Volume
$\dot{W}$	[W]	Power

Greek symbols

η	[%]	Efficiency

Subscripts

cf	Cooling fluid
ec	Exhaust closed
eo	Exhaust open
ex	Exhaust
exp	Expander
hf	Heating fluid
in	Incoming
is	Isentropic
r	Refrigerant
su	Suction
th	Theoretical
tot	Total
ic	Inlet closing

INTRODUCTION

The climate and energy policy adopted by the European council in 2014 sets out to achieve a reduction of at least 40 % in greenhouse gas emissions by 2030 compared to 1990 levels and an improvement of 20 % in energy efficiency, with a view to achieving 30 % [1]. The increasing growth of renewable energy requires flexible, low-cost and efficient electrical storage systems to balance the mismatch between energy supply and demand. In a Carnot battery electric energy is stored as thermal energy when the electricity generation is abundant. The conversion from electricity to thermal energy is done with a power-to-heat system. This energy is later recovered during discharge when the electricity demand is higher than the production. This is done by a heat-to-power system with a suitable power cycle like an organic Rankine cycle (ORC) [2].

The expander in an ORC system is a critical component that affects the investment cost and overall performance of the ORC system. Expanders can be classified into two groups: volumetric expanders (displacement expanders) and turbo-expanders [3]. For small scale expanders, as in this work, volumetric machines are seen as the most advantageous compared to turbo machines [4]. Among the volumetric expanders most attention goes to single screw and scroll expanders [5, 6], but also twin screw [7], vane [8] and piston expanders have been used [3].

Volumetric expanders are characterized by its internal built-in volume ratio and the internal pressure ratio of the expansion process. During this process several losses occur, these include: under- or over-expansion, pressure drops, ambient heat transfer, leakages and friction. Under- or over-expansion losses are due to a mismatch between the built-in volume ratio of the expander compared to the pressure ratio imposed to the machine. For under-expansion, the external volume ratio over the expander is higher than its built-in volume ratio. The pressure p_{int} in the expansion chambers at the end of the expansion process is higher than the pressure p_{ex} at the expander exhaust. During under expansion the full potential of the expansion process is not used. In contrast, for over-expansion, the volume ratio over the expander is lower than its built-in volume ratio. In this mode, the pressure p_{int} is lower than the pressure p_{ex}. With the exhaust stroke work is needed to compress the working fluid back to

higher pressure and work is lost. It is crucial to match the external pressure ratio, which depend on the operating conditions of the ORC machine, with the internal pressure to minimize losses. This will represent the best isentropic efficiency of the expander [9]. Besides changing the expander speed in order to find this optimal operating point the losses can also be minimized by an adequate timing of the inlet/admission valve and outlet/exhaust valve [3]. The valves used for admission and exhaust of the working fluid are a potential source of losses and have to be designed and controlled carefully because they have a significant effect on the performance of the reciprocating expander [3]. With respect to optimizing the performance of an ORC system this study presents experimental results of the performance of a 10 kWe ORC prototype with a reciprocating piston expander with variable valve inlet timing and hence variable volume ratio.

EXPERIMENTAL SET-UP

Equipment

In the framework of the European Chester Horizon2020 project a 10 kWe ORC has been designed and built for integration in a Carnot battery with a high temperature heat pump and latent heat thermal energy storage with a PCM melting temperature of 133 °C [10]. As such, it is designed to work with low heat source temperatures (120 – 140 °C) and uses a new low GWP environmentally friendly working fluid R1336mzz(E). A schematic of the component lay out and the measuring equipment and picture of the installation is given in Figures 1Figure 2 and 2, respectively.

The volumetric piston expander used has a maximum swept volume of 511 cm³ and a maximum rotational speed of 1500 rpm. The rated electrical power output of the expander, as indicated by the manufacturer, is 15.5 kWe and can operate at a maximum inlet pressure and temperature of 30 bar and 215 °C. This piston has an internal variable inlet valve timing mechanism that can be manipulated to control the expansion ratio and increase the ORC flexibility to perform well under part-load conditions. The valve control and operation of the inlet valve of the expander is described in [11]. More details on the valve actuation can also be found in the work of Wronski et al. [3]. Cooling of the integrated synchronous motor is provided by a chiller (Thermoflex 10.000) with a rated capacity of 10 kWth.

A diaphragm pump (G10-X from Wanner) of 30.6 l/min capacity is used to pump the refrigerant and is capable of reaching pressures up to 69 bar at the maximum speed of 1450 rpm.

All heat exchangers used are SWEP brazed plate heat exchangers. The evaporator and the condenser are identical and of the B400TH type with 120 plates and a single pass. The evaporator is insulated with HT/ArmaFlex. The subcooler is a B28H type with 34 plates and is connected to a separate cooling loop connected to the Thermoflex chiller. This subcooler is used to ensure proper start-up of the ORC system without cavitation in the refrigerant pump by ensuring a minimum level of 5 °C subcooling at the pump inlet.

ORC pump and expander information is retrieved from variable frequency drives (VFD) which control the speed of the pump and expander and are connected to a Siemens S7-1200 PLC through PROFIBUS. Temperatures and pressures inside the ORC machine and the refrigerant mass flow rate are acquired with a National Instruments cRIO. Data capturing is done at a sampling rate of 2 Hz. Details about the measuring equipment are provided in Table 1.

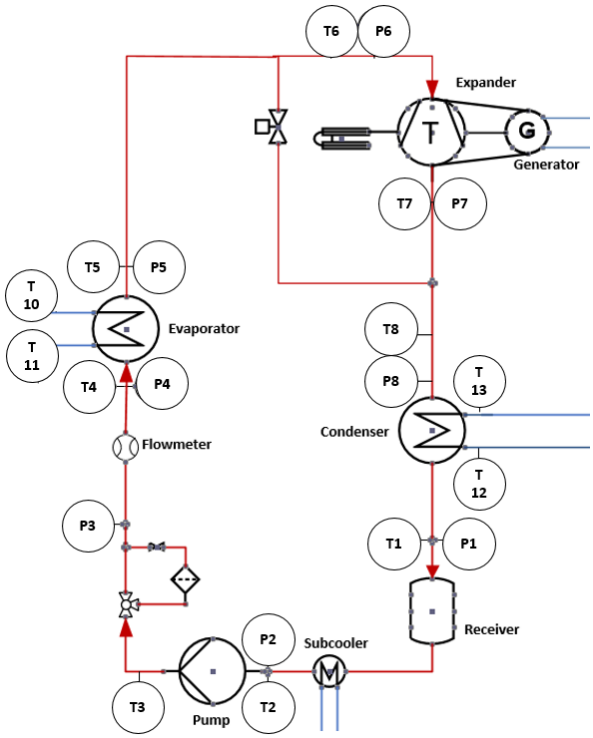

Figure 1 Schematic of the component lay-out and measuring equipment.

Figure 2 Picture of the 10 kWe prototype installation

Heating and cooling is provided with two main external loops. The heating loop consists of a Maxxtec heater made up of 10 x 25 kWe electrical heaters. Thermal oil (Therminol 66) is used as a heat transfer fluid with a maximum flow of 14 m³/h and a maximum temperature of 340 °C. The cooling loop consists of an air cooled condenser with a rated capacity of 480 kWth at 20 °C ambient and respectively water input and output temperature of 70 °C and 90 °C. The cooling medium is a mixture of water and glycol, with 27 vol% glycol. The maximum rated temperature and mass flow rate are respectively 120 °C and 20 m³/h.

Table 1 Measuring equipment and sensor uncertainties.

Measured variable	Type of sensor	Uncertainty
$\dot{m}_r$	Coriolis flow meter	± 0.15% rate ± 2.7 kg/h
$\dot{m}_{hf}$	Pressure orifice	± 1% rate
$\dot{m}_{cf}$	Ultrasonic	± 1% rate
T_{1-13}	RTD	±(0,3+0,005 * T [°C])
p_{1-7}	Absolute pressure sensor	± 0.3% span (25bar)
N_{exp}, N_{pump}, $\dot{W}_{exp}$, $\dot{W}_{pump}$	VFD	Assumed negligible

Experiments

In total 58 different steady state points have been acquired with different heat source and cold sink temperatures, different refrigerant mass flow rates and expander speeds and different expander inlet valve positions. The valve position in degrees (°) mentioned here refers to the stepper motor position installed outside the casing of the expander. This stepper motor position is controlled and changes the inlet rotary valve position and with that the inlet valve timing. The expander has been operated with four different valve positions: 140 °, 150 °, 160 °, 170 ° which corresponds to an expander load of 79 % , 86 %, 93 %, 100 %, respectively. An overview of the experimental matrix and the tested values can be found in Table 2. Steady state points are detected according to the method described in Lecompte et al. [7] and all variables are averaged over a 15 minute period.

Table 2 Experimental matrix.

Controlled parameters	Tested values
Heat source temperature (°C)	125 – 130 – 135
Heat source mass flow rate (kg/s)	3.0
Cold sink temperature (°C)	25 – 30 – 35 – 45
Cold sink mass flow rate (kg/s)	2.25
Refrigerant flow rate (kg/s)	0.4 – 0.5 – 0.6
Expander speed (RPM)	800 – 1000 – 1200 – 1400 - 1500
Expander valve position (°)	170 – 160 – 150 – 140

RESULTS AND DISCUSSION

Cycle results

The different settings can be compared through the cycle efficiency defines as:

$$\eta_{cycle} = \frac{\dot{W}_{net}}{\dot{Q}_{in}} \qquad (1)$$

The net amount of power generated by the ORC system is:

$$\dot{W}_{net} = |\dot{W}_{exp}| - |\dot{W}_{pump}| \qquad (2)$$

Heat added to the refrigerant by the heat source, i.e. through the evaporator, is calculated according to:

$$\dot{Q}_{in} = \dot{m}_r \,.\, (h_5 - h_4) \qquad (3)$$

The cycle efficiency as function of pressure ratio (PR) for the obtained steady state points is shown in Figure 3. The maximum and minimum detected cycle efficiency is 6.7% and 3.1%, respectively. The cycle efficiency increases with increasing pressure ratio over the expander. Higher pressure ratios in their turn result in higher expander power outputs as shown in Figure 4. Although the prototype has been designed for a 10 kWe output this is never reached due to PR limitations and excessive cooling of the expander generator which lowers the efficiency.

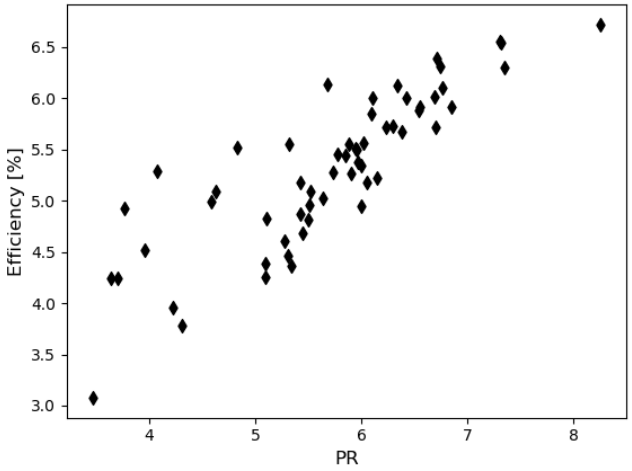

Figure 3 Cycle efficiency as function of pressure ratio

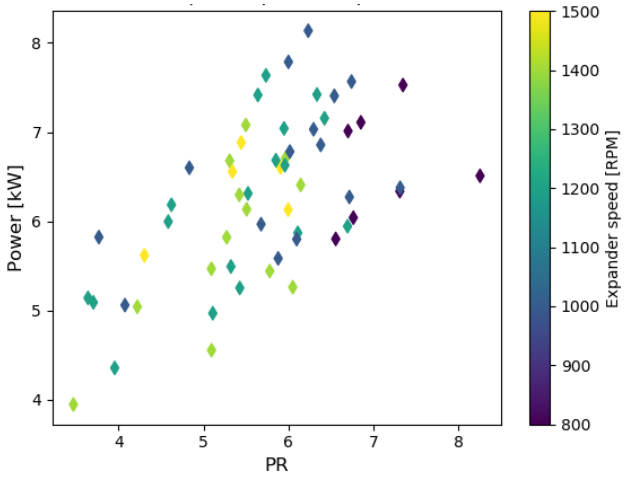

Figure 4 Expander power output as function of PR for the different tested expander speeds.

Expander performance

The expander overall isentropic efficiency is defined as the ratio of the actual enthalpy drop (derived from the measured temperature and pressure at the in- and outlet of the expander) to the isentropic enthalpy drop during the expansion process:

$$\eta_{exp,is} = \frac{h_{su} - h_{ex}}{h_{su} - h_{ex,is}} \qquad (4)$$

where h_{su} is the expander supply enthalpy, h_{ex} the expander exhaust enthalpy and $h_{ex,s}$ the exhaust enthalpy following an isentropic expansion.

In more practical form the isentropic efficiency expresses how close the power generated by the actual expansion process approximates the power of an isentropic process.

$$\eta_{exp,is} = \frac{\dot{W}_{exp}}{\dot{W}_{exp,is}} \qquad (5)$$

With:

$$\dot{W}_{exp,is} = \dot{m}_r \,.\, (h_6(T_6, p_6) - h_{7,is}(p_7, s_6)) \qquad (6)$$

Where: $s_6 = f(T_6, p_6)$

Figure 5 and Figure 6 show the results of the isentropic efficiency as function of the pressure ratio and the expander speed, respectively, for the 160 ° inlet valve position. The effect of refrigerant mass flow rate on the isentropic efficiency is negligible with only an absolute 0.14% increase on the maximum isentropic efficiency from 0.4 to 0.5 kg/s for the 150 ° valve position. Similarly, the effect of the heat source temperature is low with an increasing heat source temperature from 125 to 135°C the absolute maximum isentropic efficiency decreases with 1.2 %.

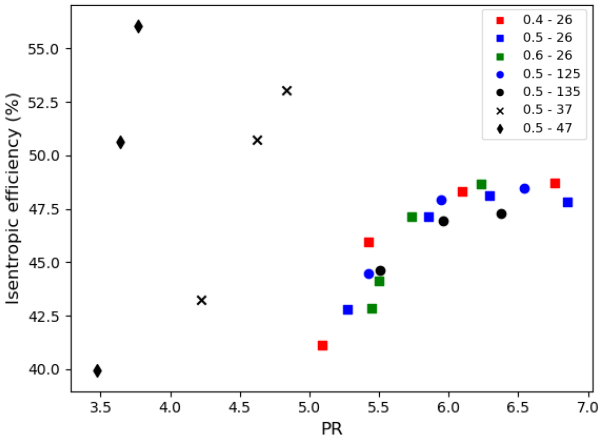

Figure 5 Expander isentropic efficiency as function of PR with the inlet valve in 160 ° position. The legend indicates first the refrigerant mass flow rate (kg/s) and then the cold sink temperature or hot source temperature (°C).

On the other hand the cold sink temperature shows the greatest effect on the isentropic efficiency. The cold sink temperature defines the condensing temperature and pressure inside the condenser so the effects seen are the result of changing expander outlet pressures. Higher expander outlet pressures result in lower pressure ratios but instead of a single continuous curve for $\eta_{exp,is} = f(PR)$ different curves are obtained for different expander outlet pressures. From Figure 6 it can also be seen that for increasing cold fluid inlet temperatures (so increasing expander outlet pressure) at constant expander speed decreases the pressure ratio but increases the isentropic efficiency. Although not shown, increasing the valve position results in a lower optimal PR. This also reflects in the fact that when the valve position is increased the inlet valve closing volume increases and hence the built-in volume ratio becomes smaller. Lower volume ratios result in lower internal expander pressures after the expansion process and hence lower optimal PR.

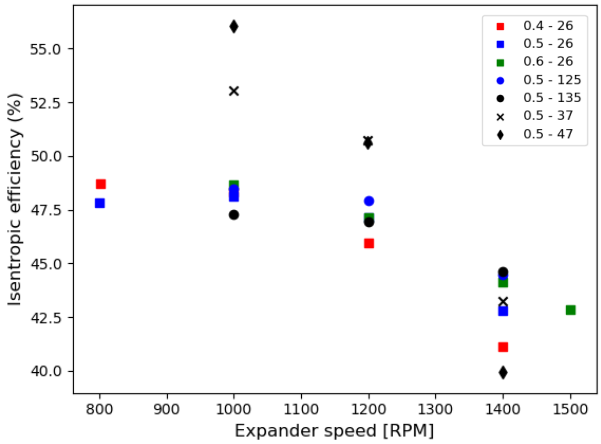

Figure 6 Expander isentropic efficiency as function of expander speed with the inlet valve in 160 ° position. The legend indicates first the refrigerant mass flow rate (kg/s) and then the cold sink temperature or hot source temperature (°C).

As most of the experiments have been conducted with a cold sink temperature of 26 - 28 °C this data clearly shows that the isentropic efficiency increases with increasing PR with an optimal PR > 6. Moreover, each expander load (or valve position) has a specific expansion ratio which reflects to an optimal PR over the expander and maximizes the energy output at an optimum isentropic efficiency. This optimal PR usually corresponds to expander speeds between 1000 – 1200 RPM. The optimum PR for cooling fluid temperatures other than 26 - 28 °C cannot be seen in the current available experimental data and will be work for the future. In the current prototype a valve position of around 150 ° gives the highest isentropic efficiencies and also the highest cycle efficiencies. This can be seen in Figure 7 where the expander power output is shown for different valve positions with similar process conditions. The expander power output increases on average with 12.4% from a 170 ° valve position to the optimal 150 ° valve position. Note that the lower expander speeds are not shown in Figure 7 because these were not tested at these process conditions due to pressure restrictions.

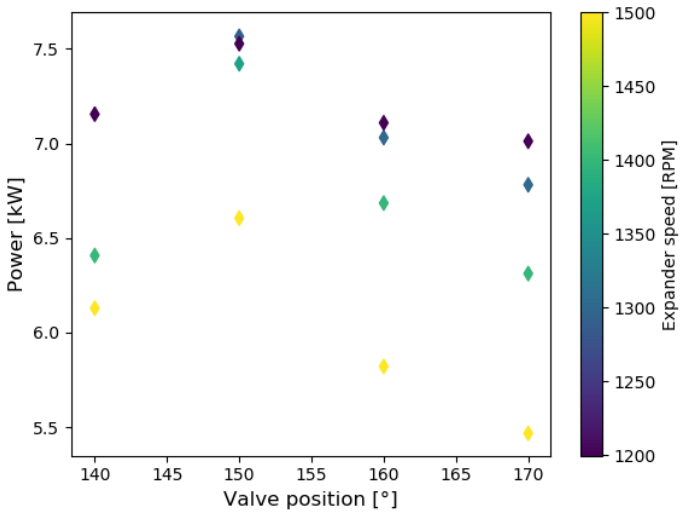

Figure 7 Expander power output as function of the expander inlet valve position for different expander speeds. Process conditions are similar for all data points with a 26 °C cold sink temperature and 130 °C heat source temperature and 0.5 kg/s refrigerant mass flow rate.

Another key parameter for the volumetric performance of a positive displacement expander is the volumetric efficiency or filling factor (FF), evaluated as:

$$FF = \frac{\dot{m}}{\dot{m}_{th}} \qquad (7)$$

with $\dot{m}$ the actual measured mass flow rate and $\dot{m}_{th}$ theoretical mass flow rate admitted by the expander.

The theoretical volume entering into the cylinder is the difference between the masses in the cylinder when the inlet valve closes and the exhaust valve closes. The theoretical mass flow rate is then given by:

$$\dot{m}_{th} = N.(V_{ic}.\rho_{ic} - V_{ec}.\rho_{ex}) \qquad (8)$$

Where ρ_{ic} is the density of the fluid at the end of the supply process and ρ_{ex} is the exhaust fluid density. ρ_{ic} is different from the density at the supply, ρ_{in}, because of the mixing of the new fluid charge and the fluid remaining in the clearance volume, V_0. As ρ_{ic} is difficult to determine ρ_{in} will be used and is calculated as $f(T_6, p_6)$. However, since V_{ec} is unknown in this case and the mass encountered in the cylinder at the end of the compression phase is generally relatively low it is often neglected.

Figure 8 and Figure 9 show the results of the filling factor as function of the pressure ratio and the expander speed, respectively. The general trend is that the volumetric efficiency increases with increasing PR (at constant cooling fluid inlet temperatures) and with decreasing expander speed. Similar to the isentropic efficiency curves, changing the cooling fluid inlet temperature results in different curves instead of one continuous curve. Furthermore the actual refrigerant mass flow rate also affects the filling factor with lower flowrates resulting in a higher filling factors.

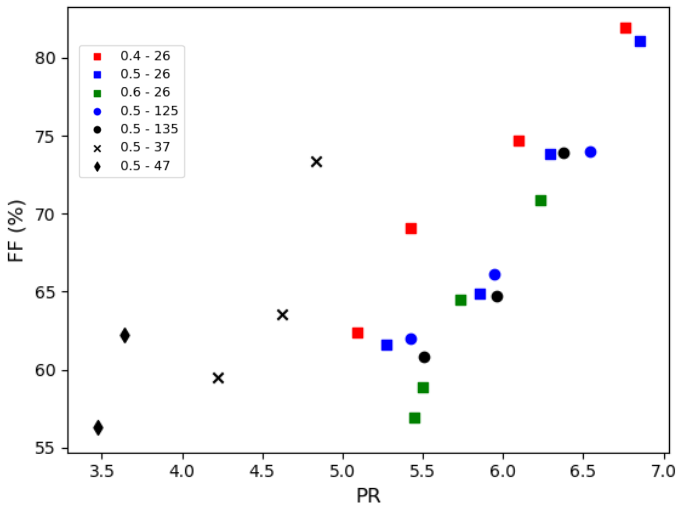

Figure 8 Expander filling factor as function of PR with the inlet valve in 160 ° position, the legend indicates first the refrigerant mass flow rate (kg/s) and then the cold sink temperature or hot source temperature (°C).

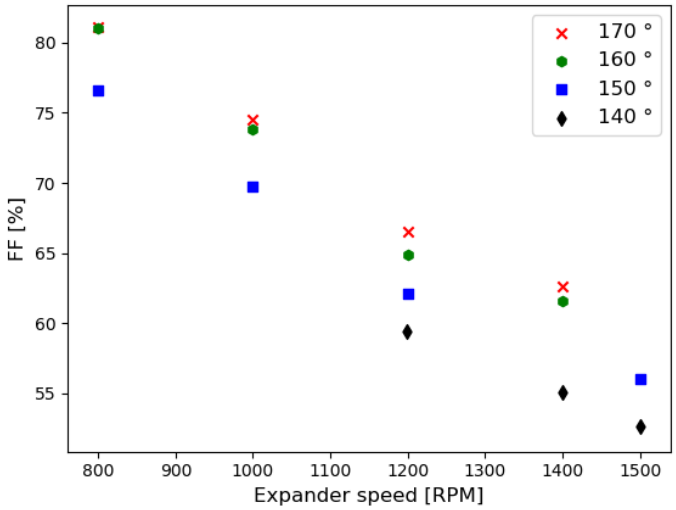

Figure 9 FF as function for different expander inlet valve positions. Process conditions for all datapoints are similar with a 26 °C cold sink temperature and 130 °C heat source temperature and 0.5 kg/s refrigerant mass flow rate.

On the other hand, the volumetric efficiency decreases with increasing rotational speed. With higher rotational speeds, the intake period shortens. This shortening causes an increase of the supply pressure drop that leads to lower working fluid densities in the working chamber after the pressure drop compared to the density at the entrance of the expander. Eventually this means a reduction of the admitted mass in the chamber than theoretically calculated. In addition, this pressure drop also affects leakage flows, leading to a reduction in the volumetric efficiency according to Rijpkema et al. [12]. The combined effect of pressure drop, leakage flows and additionally the clearance volume, valve timing, internal and external heat losses and mechanical losses could be estimated by the approach followed in Rijpkema et al. [12] and Lemort et al. [13].

CONCLUSION

Experimental results on the overall isentropic efficiency and the volumetric performance in terms of filling factor have been presented. The effects of variable valve inlet timing on the performance of a reciprocating piston expander on an ORC charged with R1336mzz(E) has been demonstrated. By using an expander with inlet valve timing the operating conditions could be matched with the heat source and heat sink temperatures in order to work at maximum efficiency. Each expander valve position comes with a best operating point in terms of efficiency. In general this best efficiency point relates to expander speeds between 1000 to 1200 RPM for the test conditions on this work. These lower expander speeds result in higher pressure ratio's. The higher expander speeds result in higher pressure drops at the inlet of the expander and eventually lower efficiencies. Besides the expander speed and pressure ratio also the condensing pressure highly influences the expander performance. Higher condensing pressures directly result in lower pressure ratios when the expander inlet pressure is kept constant. Instead of having one continuous efficiency curve multiple efficiency curves exist each corresponding to a given condenser pressure. Higher condenser pressures result in higher isentropic efficiencies. Although the expander efficiencies are highest with higher condenser pressures, the overall cycle efficiency increases with low condenser pressures as more work can be produced with higher pressure ratios over the expander. Choosing the optimal working conditions of the expander for given process conditions will be a trade off in terms of working at highest possible expander inlet pressures by changing the inlet valve timing and working at optimal expander efficiency..

ACKNOWLEDGEMENTS

This work has been partially funded by the grant agreement No. 764042 (CHESTER project) of the European Union's Horizon 2020 research and innovation program. Xander received funding from a Ph.D. fellowship strategic basic research of the Research Foundation -Flanders (FWO) (1SD9721N).This research was supported by Flanders Make, the strategic research centre for the manufacturing industry, Belgium.

REFERENCES

1. European Parliament. *Energy policy: general principles*. 2019. Accessed October 21, 2019]; Available from: http://www.europarl.europa.eu/factsheets/en/sheet/68/energy-policy-general-principles.
2. Dumont, O., et al., *Carnot battery technology: A state-of-the-art review.* Journal of Energy Storage, 2020. **32**.
3. Wronski, J., et al., *Experimental and numerical analysis of a reciprocating piston expander with variable valve timing for small-scale organic Rankine cycle power systems.* Applied Energy, 2019. **247**: p. 403-416.
4. Ziviani, D., A. Beyene, and M. Venturini, *Advances and challenges in ORC systems modeling for low grade thermal energy recovery.* Applied Energy, 2014. **121**: p. 79-95.
5. Landelle, A., et al., *Organic Rankine cycle design and performance comparison based on experimental database.* Applied Energy, 2017. **204**: p. 1172-1187.
6. Ziviani, D., et al., *Characterizing the performance of a single-screw expander in a small-scale organic Rankine cycle for waste heat recovery.* Applied Energy, 2016. **181**: p. 155-170.
7. Lecompte, S., et al., *Experimental results of a small-scale organic Rankine cycle: Steady state identification and application to off-design model validation.* Applied Energy, 2018. **226**: p. 82-106.
8. Badr, O., et al., *Multi-Vane Expanders as Prime Movers for Low-Grade Energy Organic Rankine-Cycle Engines.* Applied Energy, 1984. **16**(2): p. 129-146.
9. Clemente, S., et al., *Bottoming organic Rankine cycle for a small scale gas turbine: A comparison of different solutions.* Applied Energy, 2013. **106**: p. 355-364.
10. Pillai, A., et al. *Performance analysis of an organic rankine cycle for integration in a Carnot battery*. in *5th International Seminar on ORC Power Systems*. 2019. Athens, Greece: The National Technical University of Athens (NTUA).
11. Risla, H., *Pulse-width-regulating valve*. 2014.
12. Rijpkema, J., et al., *Experimental investigation and modeling of a reciprocating piston expander for waste heat recovery from a truck engine.* Applied Thermal Engineering, 2021. **186**(116425).
13. Lemort, V., et al., *Testing and modeling a scroll expander integrated into an Organic Rankine Cycle.* Applied Thermal Engineering, 2009. **29**(14-15): p. 3094-3102.